

Technical requirements and optical design of the Hi-5 spectrometer

Dandumont, C. ; Mazzoli, A. ; Laborde, Victor ; Laugier, Romain ; Bigioli, A. ; Garreau, G. ; Gross, S.; Ireland, M. ; Loicq, J.J.D.; More Authors

DOI

[10.1117/12.2627939](https://doi.org/10.1117/12.2627939)

Publication date

2022

Document Version

Final published version

Published in

Optical and Infrared Interferometry and Imaging VIII

Citation (APA)

Dandumont, C., Mazzoli, A., Laborde, V., Laugier, R., Bigioli, A., Garreau, G., Gross, S., Ireland, M., Loicq, J. J. D., & More Authors (2022). Technical requirements and optical design of the Hi-5 spectrometer. In A. Mérand, S. Sallum, & J. Sanchez-Bermudezv (Eds.), *Optical and Infrared Interferometry and Imaging VIII* (Vol. 12183). (Proceedings of SPIE; Vol. 12183). SPIE. <https://doi.org/10.1117/12.2627939>

Important note

To cite this publication, please use the final published version (if applicable).
Please check the document version above.

Copyright

Other than for strictly personal use, it is not permitted to download, forward or distribute the text or part of it, without the consent of the author(s) and/or copyright holder(s), unless the work is under an open content license such as Creative Commons.

Takedown policy

Please contact us and provide details if you believe this document breaches copyrights.
We will remove access to the work immediately and investigate your claim.

PROCEEDINGS OF SPIE

[SPIDigitalLibrary.org/conference-proceedings-of-spie](https://spiedigitallibrary.org/conference-proceedings-of-spie)

Technical requirements and optical design of the Hi-5 spectrometer

C. Dandumont, A. Mazzoli, V. Laborde, R. Laugier, A. Bigioli, et al.

C. Dandumont, A. Mazzoli, V. Laborde, R. Laugier, A. Bigioli, G. Garreau, S. Gross, M. Ireland, H.-D. Kenchington Goldsmith, L. Labadie, M.-A. Martinod, G. Raskin, A. Sanny, J. Loicq, D. Defrère, "Technical requirements and optical design of the Hi-5 spectrometer," Proc. SPIE 12183, Optical and Infrared Interferometry and Imaging VIII, 121831Y (26 August 2022); doi: 10.1117/12.2627939

SPIE.

Event: SPIE Astronomical Telescopes + Instrumentation, 2022, Montréal, Québec, Canada

Technical requirements and optical design of the Hi-5 spectrometer

C. Dandumont^{a,g,*}, A. Mazzoli^{a,g}, V. Laborde^{a,g}, R. Laugier^b, A. Bigioli^b, G. Garreau^b, S. Gross^c, M. Ireland^d, H.-D. Kenchington Goldsmith^d, L. Labadie^e, M.-A. Martinod^b, G. Raskin^b, A. Sanny^e, J. Loicq^{f,g}, and D. Defrère^b

^aCentre Spatial de Liège, Université de Liège, Avenue Pré-Aily, 4031 Angleur, Belgium

^bInstitute of Astronomy, KU Leuven, 200D Celestijnenlaan, Leuven, Belgium

^cMacquarie University, Australia

^dThe Australian National University, Australia

^eUniversität zu Köln, Germany

^fDelft University of Technology, Netherlands

^gUliege, Belgium

ABSTRACT

Hi-5 is a proposed L' band high-contrast nulling interferometric instrument for the visitor focus of the Very Large Telescope Interferometer (VLTI). As a part of the ERC consolidator project called SCIFY (Self-Calibrated Interferometry For exoplanet spectroscopy), the instrument aims to achieve sufficient dynamic range and angular resolution to directly image and characterize the snow line of young extra-solar planetary systems.

The spectrometer is based on a dispersive grism and is located downstream of an integrated optics beam-combiner. To reach the contrast and sensitivity specifications, the outputs of the I/O chip must be sufficiently separated and properly sampled on the Hawaii-2RG detector. This has many implications for the photonic chip and spectrometer design. We present these technical requirements, trade-off studies, and phase-A of the optical design of the Hi-5 spectrometer in this paper. For both science and contract-driven reasons, the instrument design currently features three different spectroscopic modes (R=20, 400, and 2000).

Designs and efficiency estimates for the grisms are also presented as well as the strategy to separate the two polarization states.

Keywords: interferometry, nulling, exoplanets, astronomy, spectrometer, optical design

1. HI-5 : A NULLING INTERFEROMETER FOR THE VLTI

Hi-5 is part of the Asgard instrument suite (BIFROST, a Y/J/H-band combiner optimized for high spectral resolution, Heimdallr, a high-sensitivity K-band fringe tracker, and Hi-5/VIKING) which seeks to be installed at the visitor focus of the Very Large Telescope Interferometer (VLTI). It will be the first nulling instrument on the VLTI, and the first long-baseline nulloer in the Southern hemisphere. It is designed for the L'-band (3.5-4.0 μm), a sweet spot to image young planetary systems.¹

Hi-5 is optimized for high-contrast interferometry, with a main scientific focus on giant exoplanets characterization and formation, protoplanetary disks around young stars, and the prevalence and nature of exozodiacal dust. A survey of nearby young stars is planned with the ATs and follow-up spectroscopic observations with the UTs. Thanks to the long-baseline of the VLTI and the ongoing GRAVITY+ facility upgrade, the gain in sensitivity (10^{-5} in contrast) and spatial resolution compared to current instruments² will allow us to directly image the snow line where most giant exoplanets are located^{3,4} (around 2.7 AU for a solar-like star⁵) (see Dandumont et al. at this conference + in prep.).

Further author information: Colin Dandumont, colin.dandumont@uliege.be

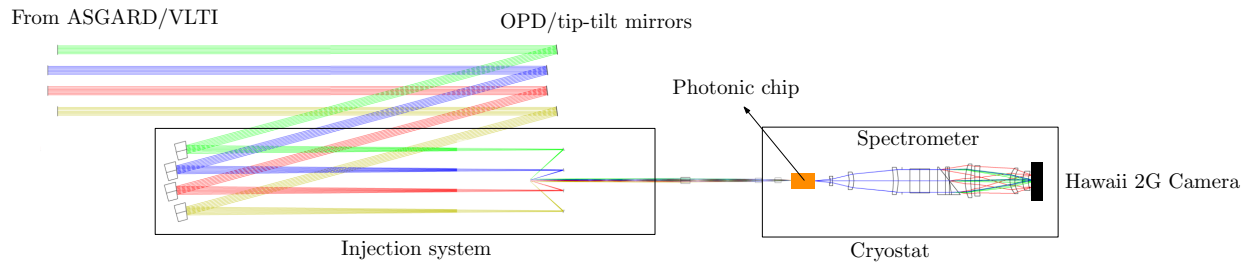


Figure 1: Current design of the Hi-5 instrument. The four beams comes from the VLTI telescopes and are injected, after tip/tilt and phase control, into the beam combiner. The spectrometer is located at the end, in a cryostat.

Figure 1 represents the current design of the instrument. The four VLTI inputs are first reduced by the Heimdallr fringe tracker (part of the Asgard suite). Then, these inputs are injected into a photonic chip to do the beam combination (double Bracewell - Angel & Cross). The injection system is developed by KU Leuven and has strict requirements on alignment ($< 1\%$ in relative intensity error), polarization (high degree of symmetry), phase control, and achromatism (see Garreau et al. at this conference). The beam combiner chip is manufactured in GLS glass at Macquarie University and tested in Cologne (see Sanny et al. at this conference). From the four VLTI inputs, eight outputs are created (2 destructive, 2 constructive, and 4 photometric). A spectrometer, the subject of this paper, is located just afterward. The polarization is split by a Wollaston and the light is spectrally dispersed on a Hawaii 2RG[®] camera. The photonic chip and the spectrometer are placed in a vacuum cryogenic environment (< 100 K).

This paper describes the spectrometer. It is organized as follows. Section 2 is dedicated to the scientific requirements and specifications, followed in Sec. 3 by a presentation of the spectrometer optical design. A refractive design is selected and the design of the dispersive elements, grisms in this case, are presented in Sec. 5. In Sec. 4, the responses to requirements are given and how it affects the general design. Conclusions are given in Sec. 6.

2. SPECIFICATIONS & REQUIREMENTS

The Hi-5 science cases lead to very stringent specifications and requirements. They are derived from our performance simulator tool, SCIFYSIM (see Laugier et. al at this conference + in prep.). The GRAVITY spectrometer was selected as a baseline. It operates in K-band ($1.95 - 2.45 \mu\text{m}$) at the VLTI, and also provides three spectral resolutions ($R = 22, 530, \text{ and } 4500$).⁶

The Hi-5 requirements are presented in Tab. 1. The spectrometer will operate in L'-band ($3.5 - 4.0 \mu\text{m}$) in a cryogenic vacuum environment at a temperature of < 100 K and will propose three spectral resolutions ($R = 20, 40, \text{ and } 2000$). Each output of the integrated optic beam combiner is split in polarisation before the grism thanks to a Wollaston prism.

For high-contrast observations, cross-talk between destructive output and constructive outputs should be minimized. Figure 2 shows the collected light for several sizes of the PSF (PSF is centered between the pixels). It shows that with 2×2 pixels, the cross-talk is around 5×10^{-3} and if we add a pixel (so a 3×3 pixels square), it goes down to 10^{-3} . The cross-talk is directly related to the spacing between each output of the beam combiner.

3. SPECTROMETER OF THE HI-5 INSTRUMENT

Figure 3 shows the optical design for the three different spectral resolutions ($R = 20, 400, \text{ and } 2000$). The inputs are the 8 outputs of the beam combiner (left of Fig. 3). The numerical aperture of the collimator is related to the beam combiner. This collimator is made of three spherical lenses, the first one being in CaF_2 and the two others in ZnSe . Both materials are transparent in the L'-band. To split the polarization, a Wollaston is positioned just after. It could be removed without changing the focal plane (collimated beam + parallel faces). Three germanium grisms were developed and optimized (see Sec 5). They will be mounted on a wheel mechanism.

General	
operating wavelength	3.5 - 4.0 μm
operating temperature	< 100 K
Injection unit	
number of optical input channels	4 (4 telescopes)
Beam combiner	
number of optical output channels	8 (4 photometric, 2 constructive, and 2 destructive)
linear spacing of the outputs	125 μm
fiber core radius of the outputs channels	
intensity distribution of output channels	gaussian
Polarimetric capabilities	
wollaston prism	
arrangement of polarised spectra with respect to spectral dispersion	perpendicular
Spectral resolutions	
minimum spectral resolution	$R = 20$
intermediate spectral resolution	$R = 400$
maximal spectral resolution	$R = 2000$
Detector	
detector array	HAWAII 2RG [®]
pixel size	18 x 18 μm^2
useful area of pixels [width x height]	0.6 x 15.4 mm^2 (34 x 855 pixels ²)
detector temperature	< 60 K
hline Image quality	
diffraction-limited crosstalk between constructive and destructive outputs	< 10^{-3} (3 pixels spacing)
detector area to contain $\leq 90\%$ of ensquared energy $1/e^2$ flux	36 x 36 μm^2

Table 1: Optical requirements and specifications for the Hi-5 spectrometer.

A change of spectral resolution will not affect the image plane position. Since the spectrometer is inside the cryostat, a change of spectral resolution will not need any technician intervention. The imaging part is composed of three spherical lenses and one aspherical lens. They are all in ZnSe. The detector, the HAWAI 2RG[®], is located at the image plane.

4. RESPONSE TO REQUIREMENTS

4.1 Ensquared energy and constraint related to the cross-talk

Figure 4 summarises the calculation process. As stated in Tab. 1, 90% of the ensquared energy needs to fall within a 2 by 2 pixels matrix (1 pixel being 18 μm) in order to maximize efficiency. To minimize any cross-talk between the constructive and destructive outputs, they need to be separated horizontally (spatial resolution) by 3 pixels on the detector. These specifications dictate the full optical design. On the vertical axis, the spectral dimension is sampled by 3 pixels. The size of the pixel and this sampling value gives the dimension of the full spectrum (855 pixels for $R = 2000$). The Bragg's law gives (order -1) the incidence angle and the grooved period for each spectral resolution. The focal length of the imager ($f = 50$ mm) can be derived from these parameters. The specification on the ensquared energy (90 % in 2 x 2 pixels) constrains the PSF diameter. In order to validate this, the Airy disk needs to fall within 1 pixel. Figure 5 shows that indeed more than 90% of the $1/e^2$ flux of the Gaussian beam profile falls within a 2×2 pixels matrix for each spectral resolution. From the PSF diameter and the diffraction limit law, the collimator beam diameter impacting the grism is computed ($D = 28$ mm). With the numerical aperture (NA) of the beam combiner outputs being fixed, the collimator

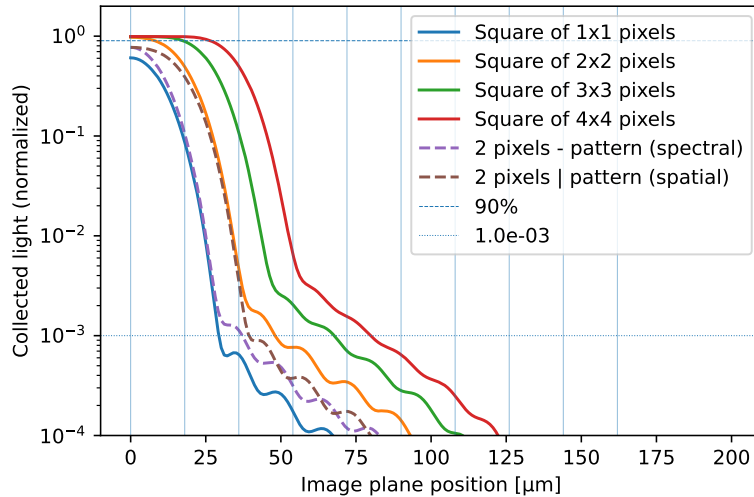


Figure 2: Collecting light (Airy pattern) for different sampling of the Point-Spread-Function in colors. PSF is centered between the pixels. 71% of collected light falls within 1 x 1 pixel and 98% within 2 x 2 pixels. One pixel is 18 μm wide.

design is constrained. One degree of freedom is the horizontal spacing between outputs. Since the cross-talk needs to be avoided between the bright and the nulled outputs, the corresponding beam combiner outputs are more separated on the chip as depicted in Fig. 6. It shows the spots arrangement on the detector for the central wavelength (3.75 μm). Bright (constructive) and nulled (destructive) outputs are indeed separated by 3 pixels while other outputs are separated by 2 pixels. Each output of the beam combiner is split in polarization. The light is spectrally dispersed on the vertical axis of the detector. It covers an area of 0.6 x 15.4 mm² or 34 x 855 pixels. It is less than GRAVITY spectrometer since Hi-5 combines 4 telescopes and creates 8 outputs that are split in polarization (8 x 2 = 16 spots). GRAVITY combines all the VLTI telescopes (6 baselines) and has 4 outputs (ABCD). Polarization is also split, which leads to 6 x 4 x 2 = 48 outputs.⁶

4.2 Polarization splitting

The Hi-5 injection system is designed (see Garreau et al. at this presentation) to have a high symmetry to avoid any change of polarization between the input beams coming from the VLTI. After the beam combination, for sensitivity, polarization should be split. Light from the VLTI has a polarization mismatch in intensity (around 10%) and s-p delay retardation. A Wollaston is therefore implemented just after the stop (see Fig. 3). Since each output is collimated and the Wollaston faces are parallel, it can be removed without impacting the optical design. In that case, the two polarizations will merge at the image plane. The angle of divergence is set to 2 degrees to have the 2 pixels separations between each polarization (Fig. 6).

During the design process, it appeared that the flux distribution at the image plane between both polarizations was not the same (50% of the output flux before the Wollaston). After analysis, the high curvature of the third and mainly the fourth lens creates an imbalance between each polarization state. It was corrected and at this state, the flux distribution is well balanced (50/50%).

4.3 Temperature effect

The spectrometer will be in a vacuum cryogenic environment (cryostat) at < 100 K during operations. It was first designed at ambient temperature. Once the cryostat temperature was fixed, the design was redefined at < 100 K. Knowing the coefficient of thermal expansion (CTE) and the change in refractive index with the temperature, the specifications at ambient temperature can be retrieved. The instrument will be built, assembled, and calibrated at ambient temperature.

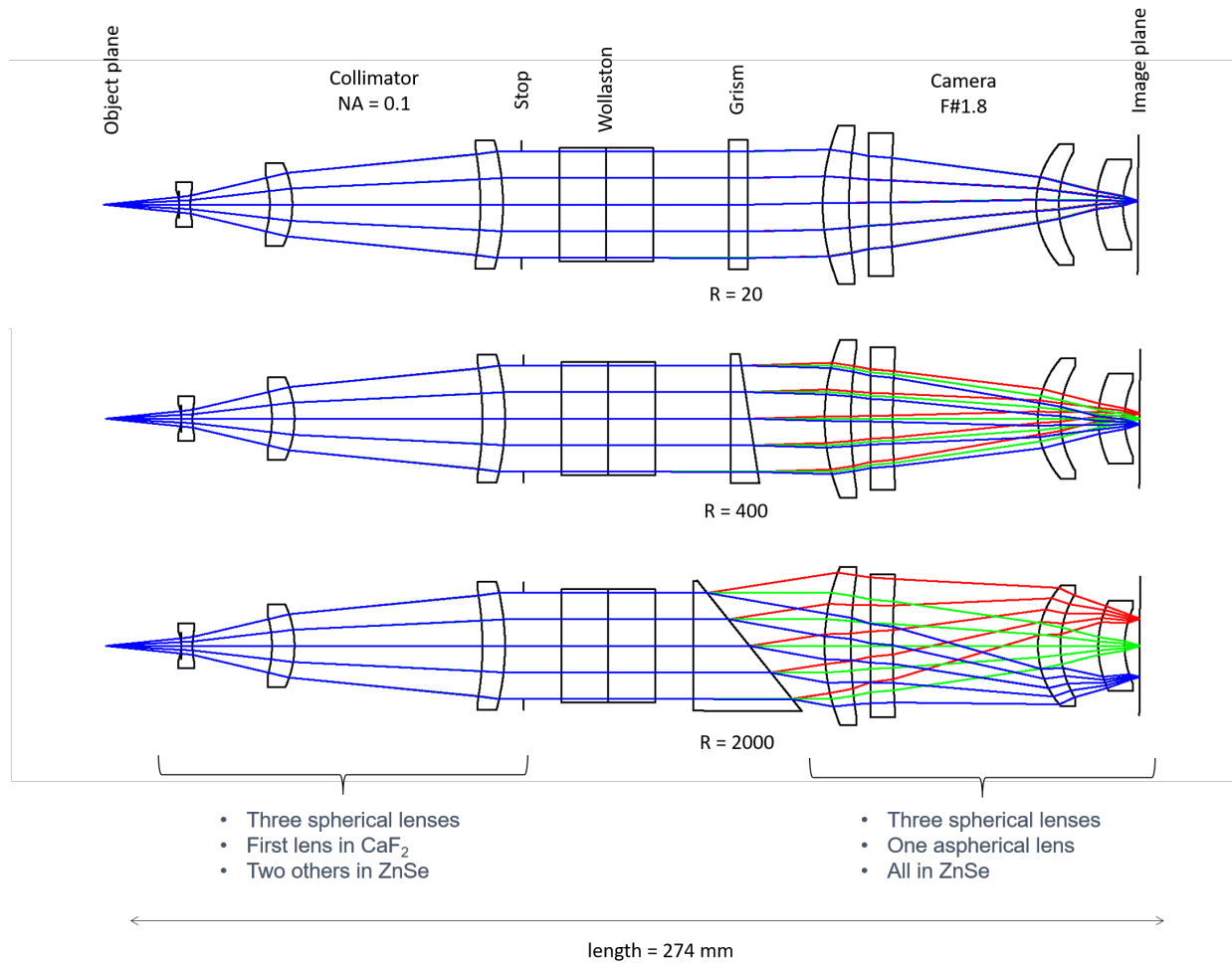


Figure 3: Side view (cut) of the spectrometer optical layout. Each spectral resolution ($R = 20, 400, \text{ and } 2000$) is depicted. Only the three germanium gratings are changed between each configuration (the focal plane is fixed). They will be mounted on a wheel mechanism.

5. GRISM DESIGN

The spectrometer has three spectral resolutions ($R = 20, 400, \text{ and } 2000$). For the gratings, ZnSe was first selected but due to the low diffraction efficiency (throughput) and encouraging results from the GRAVITY upgrade,⁷ we moved to germanium gratings. It offers a higher throughput in the operating wavelength, which is crucial for a nuller instrument.

As shown in Fig. 4, the Bragg's law will provide the optimum incidence angle and grating period to keep an in-line design.

5.1 Grism/Throughput efficiency

5.1.1 $R = 2000$ resolution

According to the optical design, the grating parameters are $T = 2.007 \mu\text{m}$ and $I = 38.661^\circ$, where T is the grating period and I the incidence angle (cf. Tab 3). Since we are considering MWIR wavelengths (from 3.5 to 4 μm), the grating features are sub-wavelength and the performance cannot be evaluated by the Scalar Theory of Diffraction (SDT). The software PCGrate[®] is used instead. It performs the rigorous Integral Equation Method

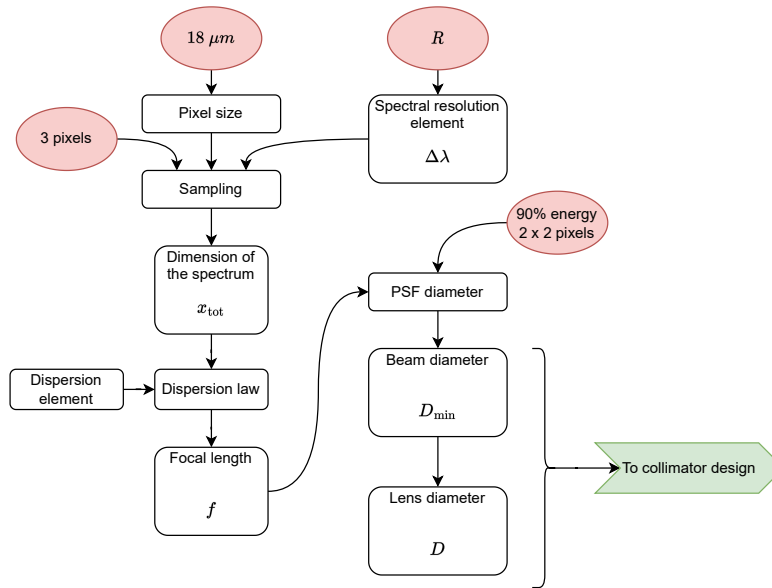


Figure 4: This flow chart summarizes the design process of the spectrometer. Red boxes represent inputs from the specifications/requirements.

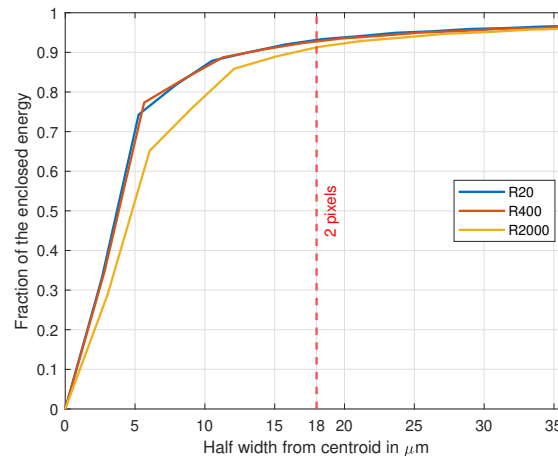


Figure 5: Encircled energy for each spectral resolution. It shows that more than 90% of the $1/e^2$ flux of the Gaussian beam profile falls within an area of 2×2 pixels (1 pixel is $18 \mu\text{m}$ wide).

to compute the diffraction efficiency for various groove profiles.⁸ Both sawtooth and blazed profiles have been considered and studied using this software. Only the blazed profile allows sufficient diffraction efficiency for the uncoated germanium grating. Figure 7 shows this diffraction efficiency according to the blaze angle, resulting from a PCGrate[®] scan study. Since the Wollaston is positioned before the grism, the polarization effect was studied and the TE, TM, and combined polarizations for order -1 are displayed.

Finally, a ridge (R) and a land (L) have been added to furthermore increase the grating efficiency while also reducing its aspect ratio and steep manufacturing edges. The resulting $R = 2000$ grating layout is depicted in Fig. 8a.

The resulting diffraction efficiency for this design is summarized in Tab. 2 (no coating).

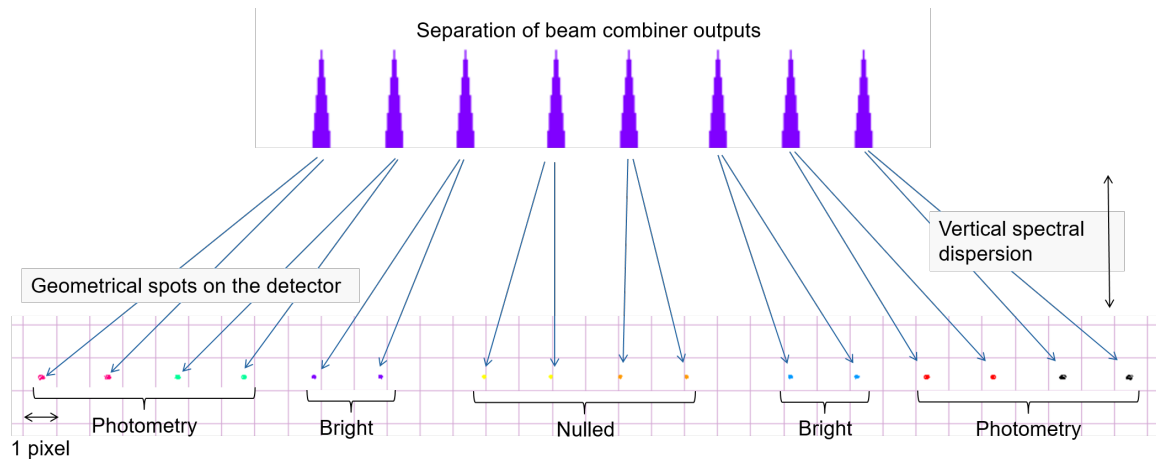


Figure 6: Geometrical spots arrangement on the detector for the central wavelength ($3.75 \mu\text{m}$). Each output of the beam combiner is split in polarization. They are separated on the detector by 2 pixels ($1 \text{ pixel} = 18 \mu\text{m}$). Bright and nulled are separated by three pixels. The light is spectrally dispersed on the vertical axis.

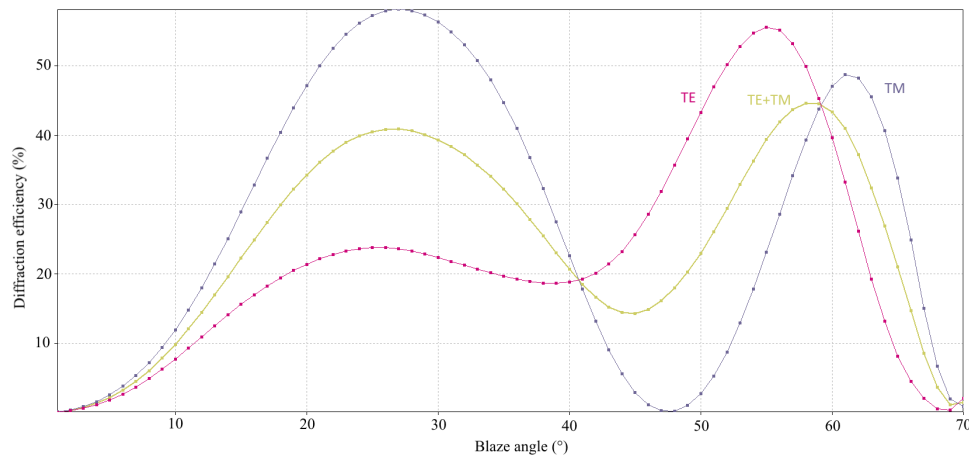


Figure 7: Diffraction efficiency for the order -1 versus blaze angle for the $R = 2000$ resolution. A 60° angle is chosen since it allows similar TE and TM efficiencies.

5.1.2 $R = 400$ resolution

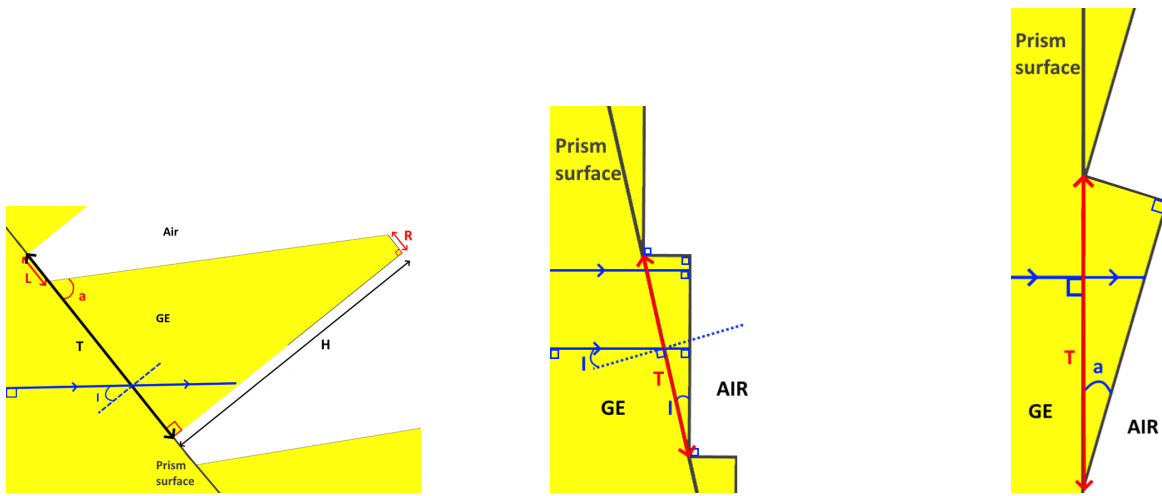
According to the optical design, the grating parameters are $T = 8.32 \mu\text{m}$ and $I = 8.664^\circ$ (cf. Tab 3). The grating period is slightly higher than the wavelength but SDT cannot be used since it requires a period at least 14 times higher than the wavelength.⁹ The software PCGrate[®] is therefore used. Similar to the Gravity design,⁶ a sawtooth profile has been selected for this resolution. The passive facet angle has the same value as the incidence angle to avoid any shadowing effect, as depicted in Fig. 8b.

The resulting diffraction efficiency for this design is summarized in Tab. 2 (no coating).

5.1.3 $R = 20$ resolution

According to the optical design, the grating parameters are $T = 170 \mu\text{m}$ and $I = 0^\circ$ (cf. Tab 3). The grating period is much more than 14 times the wavelength so SDT (validated by PCGrate[®]) provides accurate results. The sawtooth design is depicted in Fig. 8c.

The resulting diffraction efficiency is maximal for this design (taking into account the Fresnel reflections) and is summarized in Tab. 2 (no coating).



(a) $R = 2000$. Blaze angle $a = 60^\circ$. The ridge ($R = 0.2 \mu\text{m}$) and land ($L = 0.2 \mu\text{m}$) have been added to decrease the high aspect ratio and ease the manufacturing. The total groove height $H = 2.78 \mu\text{m}$.

(b) $R = 400$. Sawtooth profile. The passive facet angle is equal to the incident angle to reduce shadowing effects.

(c) $R = 20$. Sawtooth profile. SDT along with PCGrate® are used to compute the angle $a = 0.42^\circ$.

Figure 8: Grism layout for each spectral resolution.

Diffraction efficiency (%)			
λ (μm)	TE	TM	TE+TM
R = 2000			
3.5	52.2	34.7	43.5
3.75	46.6	55.8	51.2
4	41.2	49.2	45.2
R = 400			
3.5	44.5	59.2	56.8
3.75	55.4	58.3	56.8
4	54.6	56.0	55.3
R = 20			
3.5	63.0	63.0	63.0
3.75	63.7	63.7	63.7
4	62.7	62.7	62.7

Table 2: Diffraction efficiency for the three spectral resolutions. No coating is considered here.

	T [μm]	I [$^\circ$]	a [$^\circ$]
R = 2000	2.007	38.661	60
R = 400	8.32	8.664	8.664
R = 20	170	0	0.42

Table 3: Geometric parameters of the grisms for each spectral resolution.

6. CONCLUSION

We proposed the optical design of the ASGAR/Hi-5 spectrometer. It operates in L'-band and provides three spectral resolutions ($R = 20, 400, \text{ and } 2000$). It is a refractive spectrometer with three germanium gratings. Polarization is split thanks to a Wollaston. The grating design and their diffraction efficiency, in both polarization (TE and TM), are presented and discussed.

ASGAR/Hi-5 being a nulling interferometer for the visitor focus of the VLTI, high sensitivity is needed for the science cases and several outputs are generated (constructive, destructive, and photometric). Specifications and requirements are stringent, especially on the spots arrangement in the detector plane and the cross-talk between each output.

Further work will include a tolerance analysis, an optomechanical design, and a calibration study.

ACKNOWLEDGMENTS

Author contributions: AM carried out the full optical design. VL carried out the analyses of the grating and RL is in charge of SCIFYSIM. CD wrote the manuscript. JL and DD initiated and guided this project. All authors discussed the results and commented on the manuscript. SCIFY has received funding from the European Research Council (ERC) under the European Union's Horizon 2020 research and innovation program (grant agreement CoG - 866070). This project has received funding from the European Union's Horizon 2020 research and innovation programme under grant agreement No 101004719.

REFERENCES

- [1] Wallace, A. L. and Ireland, M. J., "The likelihood of detecting young giant planets with high-contrast imaging and interferometry," *Monthly Notices of the Royal Astronomical Society* **490**, 502–512 (Nov. 2019).
- [2] Defrère, D., Absil, O., Berger, J.-P., Boulet, T., Danchi, W. C., Ertel, S., Gallenne, A., Hénault, F., Hinz, P., Huby, E., Ireland, M., Kraus, S., Labadie, L., Le Bouquin, J.-B., Martin, G., Matter, A., Mérand, A., Mennesson, B., Minardi, S., Monnier, J. D., Norris, B., de Xivry, G. O., Pedretti, E., Pott, J.-U., Reggiani, M., Serabyn, E., Surdej, J., Tristram, K. R. W., and Woillez, J., "The path towards high-contrast imaging with the VLTI: the Hi-5 project," *Experimental Astronomy* **46**, 475–495 (Dec. 2018).
- [3] Fernandes, R. B., Mulders, G. D., Pascucci, I., Mordasini, C., and Emsenhuber, A., "Hints for a Turnover at the Snow Line in the Giant Planet Occurrence Rate," *The Astrophysical Journal* **874**, 81 (Mar. 2019).
- [4] Fulton, B. J., Rosenthal, L. J., Hirsch, L. A., Isaacson, H., Howard, A. W., Dedrick, C. M., Sherstyuk, I. A., Blunt, S. C., Petigura, E. A., Knutson, H. A., Behrmann, A., Chontos, A., Crepp, J. R., Crossfield, I. J. M., Dalba, P. A., Fischer, D. A., Henry, G. W., Kane, S. R., Kosiarek, M., Marcy, G. W., Rubenzahl, R. A., Weiss, L. M., and Wright, J. T., "California Legacy Survey. II. Occurrence of Giant Planets beyond the Ice Line," *The Astrophysical Journal Supplement Series* **255**, 14 (July 2021).
- [5] Ida, S. and Lin, D. N. C., "Toward a Deterministic Model of Planetary Formation. III. Mass Distribution of Short-Period Planets around Stars of Various Masses," *The Astrophysical Journal* **626**, 1045–1060 (June 2005).
- [6] Straubmeier, C., Fischer, S., Araujo-Hauck, C., Wiest, M., Yazici, S., Eisenhauer, F., Perrin, G., Brandner, W., Perraut, K., Amorim, A., Schöller, M., and Eckart, A., "The GRAVITY spectrometers: optical design and principle of operation," 773432 (July 2010).
- [7] Yazici, S., Sukegawa, T., Mayer, M., Eisenhauer, F., Okura, Y., Perraut, K., Jocu, L., Gillessen, S., Haussmann, F., Buron, A., Huber, D., Barl, L., Kravchenko, K., Pfuhl, O., Lacour, S., Lapeyrere, V., Wiezorrek, E., Ott, T., Paumard, T., Shangguan, J., Gao, F., Straubmeier, C., Guajardo, P., Riquelme, M., Pallanca, L., Genzel, R., de Zeeuw, T., Bauböck, M., Habibi, M., Rau, C., Jimenez Rosales, A., Stadler, J., Straub, O., Sturm, E., von Fellenberg, S., Widmann, F., Wieprecht, E., Eckart, A., Perrin, G., Amorim, A., Garcia, P., and Brandner, W., "GRAVITY upgrade with high-performance gratings with factor >2 enhanced throughput," in [*Optical and Infrared Interferometry and Imaging VII*], Mérand, A., Sallum, S., and Tuthill, P. G., eds., 42, SPIE, Online Only, United States (Jan. 2021).
- [8] H. Kleemann, B., "Integral equation methods from grating theory to photonics: An overview and new approaches for conical diffraction," *Journal of Modern Optics* **58**, 407 (Jan. 2011).

- [9] Pommet, D. A., Moharam, M. G., and Grann, E. B., "Limits of scalar diffraction theory for diffractive phase elements," *J. Opt. Soc. Am. A* **11**, 1827–1834 (Jun 1994).